Optimal Coordination of Mobile Sensors for Target Tracking Under Additive and Multiplicative Noises

Zaiyue Yang, *Member, IEEE*, Xiufang Shi, and Jiming Chen, *Senior Member, IEEE*

***Abstract*—In this paper, the target tracking problem is investigated for a tracking system with mobile range-only sensors. Being different from most previous studies, both additive and multiplicative noises in measurements are taken into consideration. An optimal coordination strategy, including sensor selection and sensor motion, is proposed to maximize the tracking accuracy. In particular, by fully utilizing the properties of objective function, the search space and variables of the original optimization problem can be significantly reduced. Based on this reduction, three algorithms are designed, respectively, for the following: 1) efficient selection of task sensors; 2) reduction on combinations of task sensors; and 3) efficient search of optimal sensor motion. The performance of the proposed coordination strategy is illustrated by simulations.**

***Index Terms*—Fisher information matrix (FIM), multiplicative noise (MN), range-only localization, sensor motion, sensor selection, target tracking.**

I. Introduction

With the development of wireless sensor networks, target tracking has been widely applied in many fields, e.g., surveillance, environment monitoring, military, and security; it attracts increasing research interests [1]–[9]. In most occasions, a number of sensors are deployed in the field of interest to collect positional data of the target and then transmit the data to a processing unit to perform the tracking task in a centralized or a decentralized fashion.

Tracking accuracy is one of the most important goals for system designers, which strongly depends on the relative positions between sensors and target [2], [10]. In [2], the optimal sensor placement for range-only target tracking system is analyzed, and the optimal angular configuration is derived. Reference [10] studies the optimal sensor–target geometries for range-only-, time-of-arrival-, and bearing-only-based localization and identifies the optimal sensor–target configuration for different number of sensors. Undoubtedly, by providing mobility to the sensors, the tracking accuracy can be significantly improved via sensor motion coordination. In [2], a motion strategy for the mobile sensors is designed to satisfy the optimal angular configuration, in which there is no limitation on the mobility of sensors. In [11] and [12], it is assumed that each sensor can move a given distance at each time step, and the motion strategies are designed under the constraint. Reference [13] develops a distributed flocking algorithm for multiple robots to track the estimated target and avoid collision.

On other hand, sensor selection is another important issue in target tracking problems because, in practice, only a few sensors will be activated as task sensors for tracking due to energy limitation [3], [14]–[17]. In [3], different approaches are utilized for sensor selection under different measures of information utility. References [14] and [15], respectively, provide a global and a local algorithm of selecting the task sensors of a bearing-only tracking system to maximize the tracking accuracy. In [16], an algorithm of adaptively selecting the number of task sensors is proposed.

For a range-only target tracking system, the measurement model in most existing studies [2], [11], [12] only considers additive noise (AN), resulting that the measurement error is independent of the sensor–target distance. However, the experimental data in [1] show the existence of multiplicative noise (MN), and the variance of MN is often three to four times larger than that of AN. Due to the existence of MN, the measurement error will significantly increase with the increase in sensor–target distance. Therefore, MN cannot be ignored in the design and analysis of a target tracking system. Unfortunately, the target tracking problem with MN is quite different from that with AN; thus, it cannot be treated as a simple extension of previous results.

In this paper, the target tracking problem with both additive and multiplicative noises (AMN) is investigated for mobile range-only sensors. The ultimate goal is to design an optimal sensor coordination strategy, including sensor selection and motion, to improve tracking accuracy. Following a target tracking framework similar to [1], this task can be transformed into optimizing a certain metric, which represents the localization accuracy of each step, by properly selecting sensors and adjusting their positions. Then, the optimization of such metric can be formulated as a multivariable nonlinear optimization problem.

In order to efficiently solve this optimization problem, the following efforts are contributed.

1) By exploiting the relationship between the metric and the sensor–target distance, the search space of each sensor, as well as the optimization variables associated with each sensor, can be greatly reduced. This reduction enables the following algorithmic design.
2) By utilizing the reduction of search space, two algorithms are designed to reduce, respectively, the number of possible task sensors and the number of possible sensor

Manuscript received April 11, 2013; revised June 5, 2013; accepted August 13, 2013. Date of publication September 9, 2013; date of current version January 31, 2014. This work was supported in part by 973 Program under Grant 2013CB329503 and in part by the National Natural Science Foundation of China under Grant 61004057.

The authors are with the State Key Laboratory of Industrial Control Technology, Zhejiang University, Hangzhou 310027, China (e-mail: jmchen@ieee.org).

Color versions of one or more of the figures in this paper are available online at http://ieeexplore.ieee.org.

Digital Object Identifier 10.1109/TIE.2013.2281157

combinations, such that the computational complexity is significantly simplified.

3) According to the reduction of optimization variables, an iterative algorithm is applied to efficiently solve the nonlinear optimization problem and yield the optimal motion strategy of mobile sensors.

The rest of this paper is organized as follows. Section II introduces the target motion model and the measurement model, followed by the tracking framework. Then, the metric of tracking accuracy and the optimization problem are presented in Section III. In Section IV, reductions on the search space of mobile sensors and on the number of optimization variables are presented. In Section V, the optimal sensor coordination, including the strategy of sensor selection and sensor motion, respectively, is designed. The tracking algorithm adopted in this paper is introduced in Section VI. Simulation results illustrate the performance of our proposed approach in Section VII. Section VIII concludes this paper.

II. System Description and Tracking Framework

A. Target Motion Model

The tracking problem for a single target in 2-D field is considered in this paper. Let the state of the target at time t_k be

$$X_k = [\, x_k \quad \dot{x}_k \quad y_k \quad \dot{y}_k \,]^T$$

where (x_k, y_k) stands for the position coordinates of the target, and $(\dot{x}_k, \dot{y}_k)$ denotes the target's velocity along the x- and y-axes at time t_k, respectively. A widely used near-constant-velocity model is adopted here [1], [4], which is expressed as

$$X_{k+1} = FX_k + G\epsilon_k \tag{1}$$

where

$$F = \begin{bmatrix} 1 & \Delta\mathrm{t} & 0 & 0 \\ 0 & 1 & 0 & 0 \\ 0 & 0 & 1 & \Delta\mathrm{t} \\ 0 & 0 & 0 & 1 \end{bmatrix} G = \begin{bmatrix} \frac{\Delta t^2}{2} & 0 \\ \Delta t & 0 \\ 0 & \frac{\Delta t^2}{2} \\ 0 & \Delta t \end{bmatrix}$$

and Δt is the sampling time interval. $\epsilon_k = [\epsilon_x, \epsilon_y]^T$ is the process noise, which is assumed to be uncorrelated zero-mean white Gaussian noise with its covariance $Q = \mathrm{diag}\{\sigma^2_{\epsilon_x}, \sigma^2_{\epsilon_y}\}$.

B. Measurement Model

Assume that all the range-only sensors in the target tracking system are homogeneous and that the position of each sensor is known as a prior, which is expressed in a coordinate form $(x_{i,k}, y_{i,k})$. Then, at time t_k, the true distance between the target and sensor i is

$$r_{i,k} = \sqrt{(x_{i,k} - x_k)^2 + (y_{i,k} - y_k)^2}. \tag{2}$$

In this paper, a more general measurement model with AMN [1] is used, which is expressed as

$$z_{i,k} = (1 + \omega_{i,k}) r_{i,k} + \upsilon_{i,k} \tag{3}$$

where $z_{i,k}$ stands for the measurement of sensor i; $\omega_{i,k}$ and $\upsilon_{i,k}$ represent MN and AN, respectively, which are assumed to be uncorrelated white Gaussian noise, i.e., $\omega_{i,k} \sim N(\mu_\omega, \sigma^2_\omega)$ and $\upsilon_{i,k} \sim N(\mu_\upsilon, \sigma^2_\upsilon)$. The total measurement noise is thus expressed as $n_{i,k} = r_{i,k}\omega_{i,k} + \upsilon_{i,k}$, which is still a white Gaussian noise satisfying $n_{i,k} \sim N(\mu_{i,k}, \sigma^2_{i,k})$, where

$$\mu_{i,k} = r_{i,k}\mu_\omega + \mu_\upsilon \tag{4}$$

$$\sigma^2_{i,k} = r^2_{i,k}\sigma^2_\omega + \sigma^2_\upsilon. \tag{5}$$

As a result, the measurement $z_{i,k}$ of sensor i follows a normal distribution, i.e.,

$$z_{i,k} \sim N\left(\mu_{i,k} + r_{i,k}, \sigma^2_{i,k}\right). \tag{6}$$

For a target at (x_k, y_k), the probability density function (PDF) of sensor i's measurement is obtained as

$$p(z_{i,k}|x_k, y_k) = \frac{1}{\sqrt{2\pi}\sigma_{i,k}} \exp\left[-\frac{(z_{i,k} - r_{i,k} - \mu_{i,k})^2}{2\sigma^2_{i,k}}\right]. \tag{7}$$

Remark 1: Intuitively, the mean $\mu_{i,k}$ and the variance $\sigma^2_{i,k}$ associated with sensor i are closely related to sensor–target distance $r_{i,k}$, from (4) and (5). Because of the existence of MN, the variance $\sigma^2_{i,k}$ will grow at a geometric speed with the increase in $r_{i,k}$.

C. Tracking Framework

In this paper, it is assumed that, at time t_k, there are totally N_k mobile sensors that have detected the target, which are denoted by set Ψ_k. Then, the objective is to select M (from N_k) sensors as task sensors for target tracking, which are denoted by set Ψ^M_k and $\Psi^M_k \subset \Psi_k$, and then adjust their positions to improve tracking accuracy. Due to the limited mobility of the sensor, it is assumed that $d_{i,k} \le d_{\max}$, where $d_{i,k}$ stands for the moving distance of sensor i at t_k and $d_{\max}$ is a maximal moving distance.

Similar to (6), the measurement vector of M sensors of Ψ^M_k follows an M-dimensional normal distribution, i.e.,

$$Z_k \sim N(\mu_k, C_k) \tag{8}$$

where $Z_k = [z_{1,k}, z_{2,k}, \ldots, z_{M,k}]^T$, $\mu_k = [\mu_{1,k} + r_{1,k}, \mu_{2,k} + r_{2,k}, \ldots, \mu_{M,k} + r_{M,k}]^T$, and $C_k = \mathrm{diag}\{\sigma^2_{1,k}, \sigma^2_{2,k}, \ldots, \sigma^2_{M,k}\}$. Thus, the joint PDF with M independent measurements can be written as

$$p(Z_k|x_k, y_k) = \prod_{i=1}^{M} p(z_{i,k}|x_k, y_k). \tag{9}$$

Indeed, the target tracking task can be divided into a series of localization tasks. The tracking framework is shown in Fig. 1. At t_{k-1}, the estimated state $\hat{X}_{k-1|k-1}$ and the predicted next state $\hat{X}_{k|k-1}$ are computed from measurement vector Z_{k-1}. At t_k, according to the prediction $\hat{X}_{k|k-1}$, a new set of sensors Ψ^M_k is selected and moved to proper positions, in order to obtain the measurement Z_k and localize the target accurately.

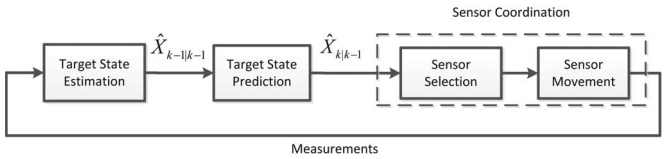

Fig. 1. Framework of target tracking and sensor coordination.

Remark 2: Note that the target tracking framework is general in a sense that it does not specify any particular algorithm for target state estimation and prediction algorithm. As our main results are derived under this framework, they can fit into any algorithm.

III. Metric of Accuracy and Problem Formulation

As previously stated, the key to improve tracking accuracy is to localize the target accurately at each time step. Here, a Fisher information matrix (FIM)-based metric will be introduced to measure localization accuracy; then, this problem can be converted into optimizing such metric at each time step.

A. FIM-Based Metric

FIM is a well-known concept in statistical signal processing and stands for the information contained in measurements [18]–[20]. A larger FIM means that we can retrieve more information from measurements and, thus, obtain more accurate estimates.

Since target localization is essential to estimate the position of the target, FIM can nicely reflect localization accuracy. Let I_k denote FIM, and from the definition in [18], we have

$$I_k = -E\left[\begin{array}{cc} \frac{\partial^2 \ln(p(Z_k|x_k,y_k))}{\partial x_k^2} & \frac{\partial^2 \ln(p(Z_k|x_k,y_k))}{\partial x_k \partial y_k} \\ \frac{\partial^2 \ln(p(Z_k|x_k,y_k))}{\partial x_k \partial y_k} & \frac{\partial^2 \ln(p(Z_k|x_k,y_k))}{\partial y_k^2} \end{array}\right]. \quad (10)$$

Since the measurement given in (8) is Gaussian with nonzero mean, mn entry of I_k can be computed as follows [18]:

$$(I_k)_{mn} = \left[\frac{\partial \mu_k(\theta_k)}{\partial(\theta_k)_m}\right]^T C_k^{-1}(\theta_k)\left[\frac{\partial \mu_k(\theta_k)}{\partial(\theta_k)_n}\right] + \frac{1}{2}\mathrm{tr}\left[C_k^{-1}(\theta_k)\frac{\partial C_k(\theta_k)}{\partial(\theta_k)_m}C_k^{-1}(\theta_k)\frac{\partial C_k(\theta_k)}{\partial(\theta_k)_n}\right] \quad (11)$$

where $\theta_k = [x_k, y_k]^T$, $m = 1, 2$, and $n = 1, 2$. Consequently

$$(I_k)_{11} = \sum_{i=1}^{M}\frac{1}{\sigma_{i,k}^4}\left\{\sigma_{i,k}^2\left[(1+\mu_\omega)\frac{x_{i,k}-x_k}{r_{i,k}}\right]^2 + \frac{1}{2}\left[2\sigma_\omega^2(x_{i,k}-x_k)\right]^2\right\}$$

$$(I_k)_{12} = (I_k)_{21} = \sum_{i=1}^{M}\frac{1}{\sigma_{i,k}^4}\left[\sigma_{i,k}^2(1+\mu_\omega)^2\frac{(x_{i,k}-x_k)}{r_{i,k}}\frac{(y_{i,k}-y_k)}{r_{i,k}} + 2\sigma_\omega^4(x_{i,k}-x_k)(y_{i,k}-y_k)\right]$$

$$(I_k)_{22} = \sum_{i=1}^{M}\frac{1}{\sigma_{i,k}^4}\left\{\sigma_{i,k}^2\left[(1+\mu_\omega)\frac{y_{i,k}-y_k}{r_{i,k}}\right]^2 + \frac{1}{2}\left[2\sigma_\omega^2(y_{i,k}-y_k)\right]^2\right\}.$$

Let $\varphi_{i,k}$ denote the angle of sensor i relative to the target and satisfy $\cos\varphi_{i,k} = (x_{i,k}-x_k)/r_{i,k}$, $\sin\varphi_{i,k} = (y_{i,k}-y_k)/r_{i,k}$, then

$$I_k = \sum_{i=1}^{M} g_{i,k}\begin{bmatrix}\cos^2\varphi_{i,k} & \cos\varphi_{i,k}\sin\varphi_{i,k} \\ \cos\varphi_{i,k}\sin\varphi_{i,k} & \sin^2\varphi_{i,k}\end{bmatrix} \quad (12)$$

where $g_{i,k}$ is a function of noise and the ith sensor–target distance

$$g_{i,k} = \frac{1}{\sigma_{i,k}^4}\left[\sigma_{i,k}^2(1+\mu_\omega)^2 + 2\sigma_\omega^4 r_{i,k}^2\right]. \quad (13)$$

Note that FIM is essentially a matrix and not convenient for further analysis. Therefore, the determinant of FIM is used as the accuracy metric, which is, in fact, the well-known D-criterion [2], [10], [21], [22]; maximizing the metric corresponds to maximizing the information obtained from the measurement. The metric $\Re_k$ is computed as follows:

$$\begin{aligned}\Re_k &= \det\{I_k\} \\ &= \left[\sum_{i=1}^{M} g_{i,k}\cos^2(\varphi_{i,k})\right]\left[\sum_{j=1}^{M} g_{j,k}\sin^2(\varphi_{j,k})\right] - \left[\sum_{i=1}^{M} g_{i,k}\cos(\varphi_{i,k})\sin(\varphi_{i,k})\right]^2 \\ &= \sum_{i=1}^{M}\sum_{j=1 j\neq i}^{M} g_{i,k}g_{j,k}\Big[\cos^2(\varphi_{i,k})\sin^2(\varphi_{j,k}) - \cos(\varphi_{i,k})\sin(\varphi_{i,k}) \times \cos(\varphi_{j,k})\sin(\varphi_{j,k})\Big] \\ &= \sum_{i=1}^{M}\sum_{j>i}^{M} g_{i,k}g_{j,k}\Big[\cos^2(\varphi_{i,k})\sin^2(\varphi_{j,k}) + \cos^2(\varphi_{j,k})\sin^2(\varphi_{i,k}) - 2\cos(\varphi_{i,k})\sin(\varphi_{i,k}) \times \cos(\varphi_{j,k})\sin(\varphi_{j,k})\Big] \\ &= \sum_{i=1}^{M}\sum_{j>i}^{M} g_{i,k}g_{j,k}\sin^2(\varphi_{i,k}-\varphi_{j,k}).\end{aligned}$$

Briefly, $\Re_k$ can be written as

$$\Re_k = \sum_{i=1}^{M}\sum_{j>i}^{M} B_{ij,k} = \frac{1}{2}\sum_{i=1}^{M}\sum_{j=1}^{M} B_{ij,k} \quad (14)$$

where

$$B_{ij,k} = g_{i,k}g_{j,k}\sin^2(\varphi_{ij,k})$$

and $\varphi_{ij,k} = \varphi_{i,k} - \varphi_{j,k}$ is the intersection angle between the line of sensor i to target and the line of sensor j to target.

B. Optimization Problem

From (14), with AMN, the localization accuracy depends on the relative positions of the target and sensors. Not only a good angular configuration but also a proper sensor–target distance lead to a good tracking performance. The objective of this paper is to design the optimal sensor coordination strategy to maximize the tracking accuracy under the constraints on task sensor number and mobility of sensors.

Let $\varphi'_{i,k}$ and $r'_{i,k}$, respectively, denote the new sensor–target angle and the distance of sensor i after movement, and $\varphi'_{i,k} \in [\varphi^{\min}_{i,k}, \varphi^{\max}_{i,k}]$. Then, the objective function can be written as

$$\max_{\Psi_k^M, \varphi'_{i,k}, r'_{i,k}} \Re_k(\varphi'_{i,k}, r'_{i,k}, \Psi_k^M)$$
$$\text{s.t.} \quad d_{i,k} \le d_{\max}, i \in \Psi_k^M. \tag{15}$$

It should be noted that, in this paper, we assume that the target is out of all the movable regions of sensors, i.e., $r_{i,k} > d_{\max}$.

Remark 3: Indeed, this optimization problem (15) can be solved straightforward, i.e., traverse all possible M-sensor combinations and search the optimal positions of M sensors for each combination. However, this undoubtedly results in very large computation because 1) there are totally $C_{N_k}^M$ combinations and 2) for each combination, there are $2M$ variables to be optimized. In order to efficiently solve this problem, the metric (14) will be fully exploited in the next section, so that the computation can be significantly reduced without degrading any tracking performance.

IV. Search Space and Variables Reduction

Since $\Re_k$ is a complicated nonlinear function of sensor–target distance and angle, the sensor coordination problem cannot be directly solved due to great computational complexity. However, it will be shown later on that by exploiting the relationship between sensor–target distance and tracking accuracy, the search space and optimization variables associated with each mobile sensor can be reduced in a large scale.

A. Properties of $\Re_k$

In (14), when the angles are fixed, i.e., $\varphi_{ij,k}$ keeps unchanged, $\Re_k$ is a strictly monotonically increasing function of $g_{i,k}$. By the derivative of g_i with respect to $r_{i,k}$, the relationship between $g_{i,k}$ and $r_{i,k}$ is obtained as follows.

1) If $2\sigma_\omega^2 < (1+\mu_\omega)^2$, $g_{i,k}$ is a strictly monotonically decreasing function of $r_{i,k}$.
2) If $2\sigma_\omega^2 \ge (1+\mu_\omega)^2$, $g_{i,k}$ is a strictly monotonically increasing function of $r_{i,k}$ when $r_{i,k} < T$ and $g_{i,k}$ is a strictly monotonically decreasing function of $r_{i,k}$ when $r_{i,k} > T$. $g_{i,k}$ achieves the maximum value $g_{\max} = (2\sigma_\omega^2 + (1+\mu_\omega)^2)^2/8\sigma_v^2\sigma_\omega^2$ at $r_{i,k} = T$, where

$$T = \sqrt{\frac{\sigma_v^2\,(2\sigma_\omega^2 - (1+\mu_\omega)^2)}{\sigma_\omega^2\,(2\sigma_\omega^2 + (1+\mu_\omega)^2)}}. \tag{16}$$

Fig. 2 illustrates the profiles of $g_{i,k}$ over $r_{i,k}$ with different MN. Then, search space and variables reduction can be conducted based on the preceding properties.

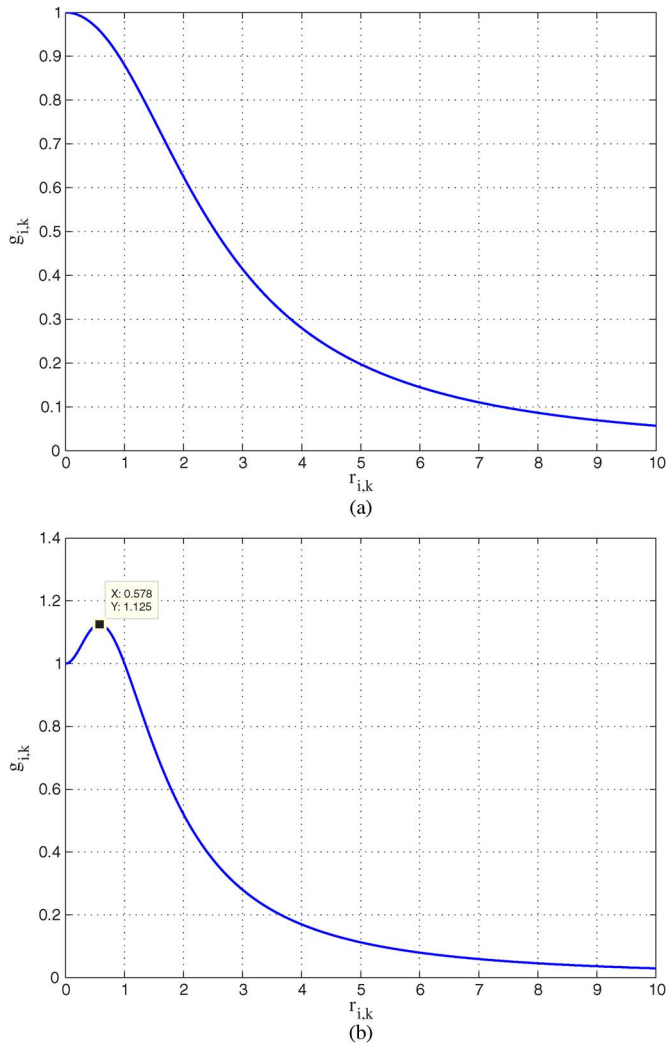

Fig. 2. Profiles of $g_{i,k}$ under two cases. Let the AN be $v_{i,k} \sim N(0,1)$ and the MN satisfy (a) $2\sigma_\omega^2 < (1+\mu_\omega)^2$ and (b) $2\sigma_\omega^2 > (1+\mu_\omega)^2$.

B. Search Space Reduction

The sensor–target distance has a different effect on the tracking accuracy under different noises. If MN satisfies $2\sigma_\omega^2 < (1+\mu_\omega)^2$, there is only one type of reduced search space, whereas if $2\sigma_\omega^2 \ge (1+\mu_\omega)^2$, there are five types of possible reduced space. The detailed analysis is given as follows.

Situation 1: $2\sigma_\omega^2 < (1+\mu_\omega)^2$. In this situation, $\Re_k$ is a strictly monotonically decreasing function of $r_{i,k}$, which means that a shorter sensor–target distance leads to better tracking accuracy. The search space of sensor i is illustrated in Fig. 3(a). Obviously, the angles on the bold curve cover the angles on the whole movable region, and in the view of sensor–target distance, the bold curve owns a better distance; as a result, tracking accuracy along the bold curve outperforms the other regions in the whole movable region.

Situation 2: $2\sigma_\omega^2 \ge (1+\mu_\omega)^2$. In this situation, there exists a distance threshold T, on which the tracking accuracy is the highest. It is better to move toward the distance threshold for sensors. The search space of each sensor is related to the current sensor–target distance $r_{i,k}$.

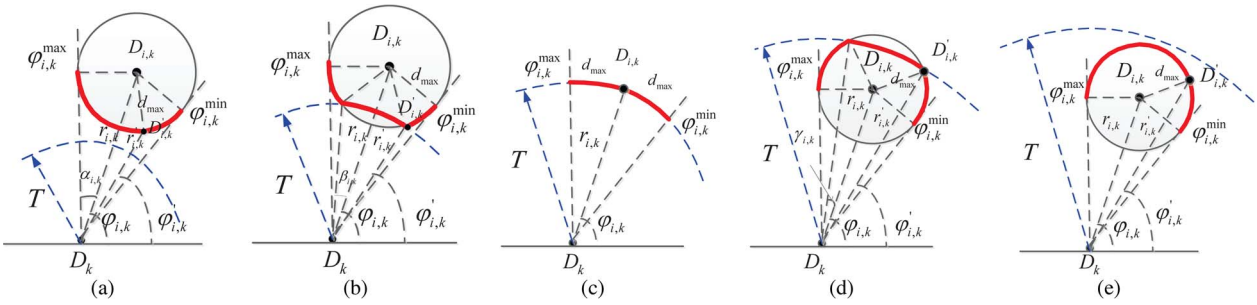

Fig. 3. Search space of sensor i under different conditions.

Case a: $r_{i,k} \geq T + d_{\max}$. The distance threshold T of sensor i to target is out of the movable region, then the reduced search space of sensor i is the shorter circular arc, which is the bold curve illustrated in Fig. 3(a).

Case b: $T < r_{i,k} < T + d_{\max}$. The distance threshold T of sensor i to target is in the circle, then the search space of sensor i is the bold curve illustrated in Fig. 3(b).

Case c: $r_{i,k} = T$. Sensor i owns the perfect distance to the target; consequently, as illustrated in Fig. 3(c), the search space of sensor i is the bold arc that is centered at the target's current position and whose radius is T.

Case d: $T - d_{\max} < r_{i,k} < T$. The distance threshold T of sensor i to target is in the circle, then the search space of sensor i is the bold curve illustrated in Fig. 3(d).

Case e: $d_{\max} < r_{i,k} \leq T - d_{\max}$. The distance threshold of sensor i to target is out of the circle, then the search space of sensor i is the longer circular arc, which is the bold curve illustrated in Fig. 3(e).

C. Optimization Variables Reduction

From the reduced search space, the ranges of $\varphi'_{i,k}$ and $r'_{i,k}$ are obtained. According to law of sines and cosines, $r'_{i,k}$ can be represented as different functions of $\varphi'_{i,k}$ under the preceding five different conditions, which cuts half of the number of optimization variables.

Situation 1: Let $D_k = (x_k, y_k)$, $D_{i,k} = (x_{i,k}, y_{i,k})$, and $D'_{i,k} = (x'_{i,k}, y'_{i,k})$, respectively, denote the position of target, the current, and the new position of sensor i. According to the law of sines, we have

$$\frac{d_{\max}}{\sin(|\Delta\varphi_i|)} = \frac{r_{i,k}}{\sin\left(\angle D_k D'_{i,k} D_{i,k}\right)} = \frac{r'_{i,k}}{\sin\left(\angle D_k D'_{i,k} D_{i,k} + |\Delta\varphi_{i,k}|\right)}$$

where $\Delta\varphi_{i,k} = \varphi'_{i,k} - \varphi_{i,k}$, and $r'_{i,k} \leq r_{i,k}$. Then, along the bold curve, $r'_{i,k}$ can be expressed as a function of $\varphi'_{i,k}$, i.e.,

$$r'_{i,k} = d_{\max} \frac{\sin\left\{\pi - \arcsin\left[\frac{r_{i,k}\sin(|\Delta\varphi_{i,k}|)}{d_{\max}}\right] + |\Delta\varphi_{i,k}|\right\}}{\sin(|\Delta\varphi_{i,k}|)} \tag{17}$$

and $\varphi'_{i,k}$ satisfies

$$\varphi_{i,k} - \alpha_{i,k} \leq \varphi'_{i,k} \leq \varphi_{i,k} + \alpha_{i,k} \tag{18}$$

where $\alpha_{i,k} = \arcsin(d_{\max}/r_{i,k})$.

Situation 2: Similarly, the relationship between $r'_{i,k}$ and $\varphi'_{i,k}$ can be summarized as follows.

Case a: It is the same as *Situation* 1.

Case b: The angle $\varphi'_{i,k}$ still yields $\varphi'_{i,k} \in [\varphi_{i,k} - \alpha_{i,k}, \varphi_{i,k} + \alpha_{i,k}]$. In addition, $r'_{i,k}$ is computed as

$$r'_{i,k} = \begin{cases} T, & \varphi_{i,k} - \beta_{i,k} \leq \varphi'_{i,k} < \varphi_{i,k} + \beta_{i,k} \\ (17), & \text{otherwise} \end{cases}$$

where $\beta_{i,k}$ is obtained by the law of cosines as

$$\beta_{i,k} = \arccos\left(\frac{r_{i,k}^2 + T^2 - d_{\max}^2}{2 r_{i,k} T}\right)$$

Case c: The length of the arc is $2d_{\max}$; as a result, $r'_{i,k}$ and $\varphi'_{i,k}$ satisfy

$$r'_{i,k} = T$$

$$\varphi_{i,k} - \frac{d_{\max}}{r_{i,k}} \leq \varphi'_{i,k} \leq \varphi_{i,k} + \frac{d_{\max}}{r_{i,k}}.$$

Case d: The angle $\varphi'_{i,k}$ still yields $\varphi'_{i,k} \in [\varphi_{i,k} - \alpha_{i,k}, \varphi_{i,k} + \alpha_{i,k}]$. $r'_{i,k}$ is expressed in the equation shown at the bottom of page, where $\gamma_{i,k}$ is obtained by the law of cosines as follows:

$$\gamma_{i,k} = \arccos\left(\frac{r_{i,k}^2 + T^2 - d_{\max}^2}{2 r_{i,k} T}\right).$$

$$r'_{i,k} = \begin{cases} T, & \varphi_{i,k} - \gamma_{i,k} \leq \varphi'_{i,k} < \varphi_{i,k} + \gamma_{i,k} \\ d_{\max} \dfrac{\sin\left\{\arcsin\left[\frac{r_{i,k}\sin\left(|\Delta\varphi_{i,k}|\right)}{d_{\max}}\right] + |\Delta\varphi_{i,k}|\right\}}{\sin(|\Delta\varphi_{i,k}|)}, & \text{otherwise} \end{cases}$$

Case e: The range of $\varphi'_{i,k}$ is $[\varphi_{i,k}-\alpha_{i,k}, \varphi_{i,k}+\alpha_{i,k}]$. The expression of $r'_{i,k}$ is

$$r'_{i,k}=d_{\max}\frac{\sin\left\{\arcsin\left[\frac{r_{i,k}\sin(|\Delta\varphi_{i,k}|)}{d_{\max}}\right]+|\Delta\varphi_{i,k}|\right\}}{\sin(|\Delta\varphi_{i,k}|)}.$$

Remark 4: The actual position of the target at time t_k is unknown. Considering that the predicted target state is accurate to a certain extent, in the design of the sensor coordination, (x_k, y_k) is replaced by the predicted target position $(x_{k|k-1}, y_{k|k-1})$.

V. Optimal Sensor Coordination

As pointed out in Remark 3, straightforward solution of (15) leads to great computation, which requires to solve $2M$-variable nonlinear optimization problem for all possible $C_{N_k}^M$ combinations of task sensors. However, by using the results in Section IV, the computation can be significantly reduced without degrading any tracking accuracy. The entire process consists of three parts: candidate task sensor selection, reduction of task sensor combinations, and optimal motion strategy.

A. Candidate Task Sensor Selection

Intuitively, it is not necessary to select all N_k sensors that detect the target as candidate task sensors because a number of sensors offer relatively poor measurements and can be excluded. The main idea is as follows. Because $\Re_k$ is a strictly monotonically increasing function of $g_{i,k}$, if the angle range of sensor i can cover the one of sensor j and $g_{i,k}>g_{j,k}$, sensor i certainly provides more informatic measurement than sensor j does; thus, sensor j should be excluded.

Let Θ_k denote the angle range of the selected candidate task sensors and $\Phi_{i,k}=[\varphi_{i,k}^{\min}, \varphi_{i,k}^{\max}]$ stand for the angle range of sensor i. The procedure of candidate sensor selection is described in Algorithm 1.

Algorithm 1:Candidate Task Sensor Selection (CTSS)

```
Sort all N_k sensors in descending order of g_{i,k}
Θ_k = 0
for i = 1, ..., N_k do
    if Θ_k ≠ [0, 2π] then
        if Φ_{i,k} ⊂ Θ_k then
            Exclude sensor i
        else
            Select sensor i as a candidate task sensor
            Θ_k = Θ_k ⋃ Φ_{i,k}
        end if
    else
        Terminate the algorithm.
    end if
end for
```

Suppose that there are L_k sensors selected as candidate task sensors via Algorithm 1, which produces $C_{L_k}^M$ possible combinations. It is notable that, usually, $C_{L_k}^M$ is much smaller than $C_{N_k}^M$, even if L_k is slightly smaller than N_k. Fig. 4 illustrates

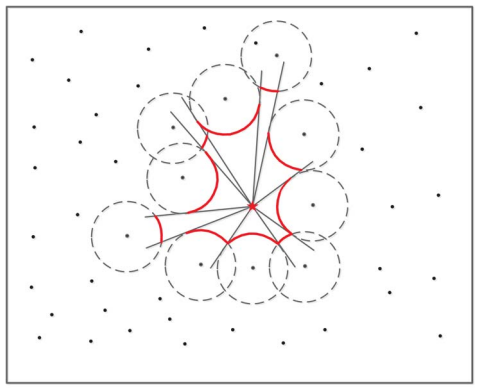

(a)

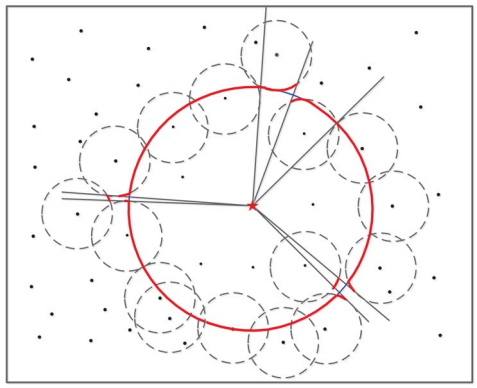

(b)

Fig. 4. Profiles of sensor exclusion under two cases of MN. (a) $2\sigma_\omega^2<(1+\mu_\omega)^2$. (b) $2\sigma_\omega^2>(1+\mu_\omega)^2$.

the selected candidate task sensors under two different cases of MN. When $2\sigma_\omega^2<(1+\mu_\omega)^2$, the candidate task sensors are close to the target, whereas when $2\sigma_\omega^2\geq(1+\mu_\omega)^2$, the candidate task sensors are close to the optimal distance threshold T. It can be seen that a number of sensors are excluded, which reduces the computational complexity in a great deal.

B. Reduction of Sensor Combination

However, $C_{L_k}^M$ may still be a large number and further simplification is needed. Clearly, if the best localization accuracy associated with combination $p=1,2,\ldots,C_{L_k}^M$ is smaller than the worst accuracy associated with combination $q=1,2,\ldots,C_{L_k}^M$, combination p can be excluded.

Let $\Re_{p,k}$ denote the metric associated with combination p at t_k, then we have

$$\Re_{p,k}^{lb}\leq\Re_{p,k}\leq\Re_{p,k}^{ub}$$

where $\Re_{p,k}^{lb}$ and $\Re_{p,k}^{ub}$ are the lower and upper bounds of $\Re_{p,k}$ obtained from (14), i.e.,

$$\begin{aligned}\Re_{p,k}^{lb}&=\sum_{i=1}^{M}\sum_{j>i}^{M}\min(B_{ij,k})\\&=\min(g_{i,k})\min(g_{j,k})\min\left(\sin^2(\varphi_{ij,k})\right)\\\Re_{p,k}^{ub}&=\sum_{i=1}^{M}\sum_{j>i}^{M}\max(B_{ij,k})\\&=\max(g_{i,k})\max(g_{j,k})\max\left(\sin^2(\varphi_{ij,k})\right).\end{aligned}$$

Therefore, combination p is excluded if

$$\Re^{ub}_{p,k} \leq \Re^{lb}_{q,k}.$$

The detailed procedure is illustrated in Algorithm.2.

Algorithm 2:Minimum–Maximum Combinations Reduction (MMCR)

1: Sort all combinations in ascending order of $\Re^{ub}_{p,k}$.
2: Find $\max\{\Re^{lb}_{1,k}, \Re^{lb}_{2,k}, \ldots, \Re^{lb}_{C^M_{L_k},k}\}$. Without loss of any generality, let it be $\Re^{lb}_{q,k}$.
3: **for** $p = 1, 2, \ldots, C^M_{L_k}$ **do**
4: **if** $\Re^{ub}_{p,k} \leq \Re^{lb}_{q,k}$ **then**
5: Combination p is excluded.
6: **else**
7: Terminate the algorithm.
8: **end if**
9: **end for**

C. Optimal Motion Strategy

Suppose there are c_k combinations remained after applying Algorithm 2. For each combination, it is necessary to find the corresponding optimal sensor motion; thus, the global optimal combination and motion of task sensors can be readily obtained by traversing all combinations.

Consider combination $p = 1, 2, \ldots, c_k$. Since the new position of each sensor is determined by $r'_{i,k}$ and $\varphi'_{i,k}$, there are $2M$ variables that need to be optimized. However, from Section IV-C, $r'_{i,k}$ can be expressed as a function of $\varphi'_{i,k}$ under different cases. Thus, considering all M sensors, $\Re_{p,k}$ can be written into a function of $\varphi'_k = [\varphi'_{1,k}, \varphi'_{2,k}, \ldots, \varphi'_{M,k}]^T$ according to (13) and (14). Then, the optimal sensor motion for combination p can be obtained by solving the following M-variable problem:

$$\begin{cases} \max & \Re_{p,k}(\varphi'_k) \\ s.t. & \varphi^{\min}_{i,k} \leq \varphi'_{i,k} \leq \varphi^{\max}_{i,k} \\ & d_{i,k} \leq d_{\max}, i = 1, 2, \ldots, M. \end{cases} \tag{19}$$

It turns out to be a problem of finding the optimal angle $\varphi'_{i,k}$ for each sensor under the constraints of movable distance.

Remark 5: The optimization problem described in (19) is a constrained nonlinear optimization problem in a complicated form. In addition, the angles are coupled with each other because $\varphi'_{ij,k} = \varphi'_{i,k} - \varphi'_{j,k}$ and $\varphi'_{ij,k}$ eventually affects the value of $\Re_k$ according to (14). Therefore, (19) cannot be analytically solved, and we shall resort to numerical solutions.

An iterative method introduced in [11] is applied to solve this problem, which is of low complexity and great efficiency. The basic idea is to optimize the angle one by one while keeping the others untouched. That is, for a tracking system with M sensors, at the $(l+1)$th iteration, the optimal angle of sensor i relative to the target is

$$\varphi'_{i,k}(l+1) = \underset{\varphi'_{i,k}(l+1)}{\arg\max}\, \Re_{p,k}\left(\phi_k(l+1)\phi_k(l)\right) \tag{20}$$

where $\varphi'_{i,k}(l+1) \in [\varphi^{\min}_{i,k}, \varphi^{\max}_{i,k}]$, $\phi_k(l+1) = [\varphi'_{1,k}(l+1), \varphi'_{2,k}(l+1), \ldots, \varphi'_{i,k}(l+1)]^T$, and $\phi_k(l) = [\varphi'_{i+1,k}(l), \varphi'_{i+2,k}(l), \ldots, \varphi'_{M,k}(l)]^T$.

The optimal motion strategy is summarized in Algorithm 3, which is referred as Sensor Motion Iterative Algorithm (SMIA) for simplicity.

Algorithm 3: SMIA

1: Given $\sigma^2_\omega, \mu_\omega, \sigma^2_\upsilon, \mu_\upsilon, (x_k, y_k), (x_{i,k}, y_{i,k}), i = 1, 2, \ldots, M$
2: **repeat**
3: **for** $i = 1 : M$ **do**
4: Identify the search space of sensor i according to Section IV-B.
5: Obtain the relationship between $r'_{i,k}(l+1)$ and $\varphi'_{i,k}(l+1)$ according to Section IV-C.
6: Calculate $\varphi'_{i,k}(l+1)$ according to (20).
7: **end for**
8: **until** The value of objective function keeps unchanged or the maximum number of iterations is reached.

After comparing the optimal tracking accuracy of all c_k combinations, the global optimal combination of task sensors and the corresponding motion can be finally determined. Our proposed strategy consisting of CTSS, MMCR, and SMIA will largely reduce the computational complexity, which is shown by simulations.

VI. Tracking Algorithm

In this paper, a newly proposed target tracking algorithm in [1] is applied for target state prediction and estimation. Compared with a normal tracking algorithm extended Kalman filter [4], [14], [23], it owns more stable tracking performance. It utilizes a maximum likelihood estimator to prelocate the position of the target and makes a conversion of the measurement to remove the sensing nonlinearity; then, a standard Kalman filter is used for state prediction and estimation.

A. Prelocalization

A prelocalization procedure is used to remove the nonlinearity of the measurement, and a maximum likelihood estimator is applied to find the target's position maximizing the joint PDF with M task sensors $p(Z_k|x_k, y_k)$ in (9).

Considering that the true value of $r_{i,k}$ is unknown, it is difficult to compute $p(z_{i,k}|x_k, y_k)$ in (7). Assume that the value of $z_{i,k}$ is close to $r_{i,k}$, then $\sigma^2_{z_{i,k}}$ can be approximated as $\sigma^2_{z_{i,k}} = z^2_{i,k}\sigma^2_\omega + \sigma^2_\upsilon$, which is based on the fact that a Kalman filter is insensitive to small changes in the noise covariance. Consequently, $p(z_{i,k}|x_k, y_k)$ is approximated as follows:

$$p(z_{i,k}|x_k, y_k) \approx \frac{1}{\sqrt{2\pi}\sigma_{z_{i,k}}} \exp\left[-\frac{(z_{i,k} - r_{i,k} - \mu_{i,k})^2}{2\sigma^2_{z_{i,k}}}\right]. \tag{21}$$

The maximum likelihood estimate of the target's position is

$$(\bar{x_k}, \bar{y_k}) = \underset{x_k, y_k}{\arg\min}\, f(x_k, y_k) \tag{22}$$

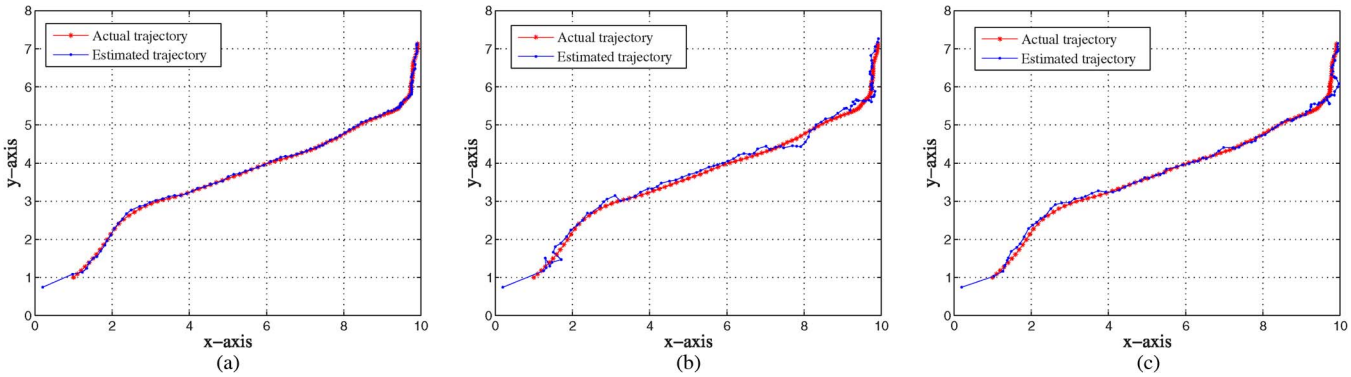

Fig. 5. Comparison between the true trajectory of the target and the estimated trajectories by three different strategies. (a) Proposed strategy. (b) Strategy of random mobile sensor selection. (c) Strategy of optimal static sensor selection.

where $f(x_k, y_k) = \sum_{i=1}^{M} (z_{i,k} - r_{i,k} - \mu_{i,k})^2 / 2\sigma_{z_{i,k}}^2$.

A Newton–Raphson iterative method is utilized to solve the aforementioned nonlinear optimization problem in [1], which is of nice convergence.

B. Kalman Filtering

After the prelocalization, the nonlinear measurement is converted into a linear model, which is expressed as

$$\bar{z}_k = \begin{bmatrix} 1 & 0 & 0 & 0 \\ 0 & 0 & 1 & 0 \end{bmatrix} X_k + \varpi_k = \bar{C} X_k + \varpi_k \tag{23}$$

where $\bar{z}_k = [\bar{x}_k, \bar{y}_k]$, and ϖ_k is the converted measurement noise. On account of the assumption that the prior PDF of the target's position is uniform, ϖ_k is zero-mean White Gaussian noise whose covariance matrix is

$$R_k = H^{-1}(\bar{x}_k, \bar{y}_k)$$

$$H(\bar{x}_k, \bar{y}_k) = \begin{bmatrix} \frac{\partial^2 f(x,y)}{\partial x^2} & \frac{\partial^2 f(x,y)}{\partial y \partial x} \\ \frac{\partial^2 f(x,y)}{\partial x \partial y} & \frac{\partial^2 f(x,y)}{\partial y^2} \end{bmatrix}_{x=\bar{x}_k, y=\bar{y}_k}.$$

Based on the linearized measurement model, the standard Kalman filter is used to estimate and predict the target state. The process of Kalman filtering is represented as follows.

1) State prediction

$$\hat{X}_{k|k-1} = F \hat{X}_{k-1|k-1}$$
$$P_{k|k-1} = F P_{k-1|k-1} F^T + G Q G^T.$$

2) State estimation

$$S_k = \bar{C} P_{k|k-1} \bar{C}^T + R_k$$
$$K_k = P_{k|k-1} \bar{C}^T S_k^{-1}$$
$$\hat{X}_{k|k} = \hat{X}_{k|k-1} + K_k (\bar{z}_k - \bar{C} \hat{X}_{k|k-1})$$
$$P_{k|k} = P_{k|k-1} - K_k S_k K_k^T \tag{24}$$

where K_k is the Kalman filter gain; $\hat{X}_{k|k-1}$ and $\hat{X}_{k|k}$ are the predicted and estimated target states, respectively; and $P_{k|k-1}$ and $P_{k|k}$ represent the corresponding error covariances.

VII. Simulation Results

Here, extensive simulations are conducted to verify the performance of the proposed coordination strategy. There are 600 sensors randomly deployed in a 140 × 120 m monitored field. The sensing range and the maximum movable distance of each sensor are set to be 10 and 0.5 m, respectively. The AN of each sensor yields $\upsilon_{i,k} \sim N(0, 0.001)$, and the MN yields $\omega_{i,k} \sim N(0, 0.001)$. During the movement of the target, the process noise is white Gaussian noise with zero mean and covariance matrix $Q = \mathrm{diag}\{1, 1\}$. The time step is set to be $\Delta t = 0.1$ s. At each time step, there are three task sensors to estimate target state, i.e., $M = 3$. The initial state of the target is $X_0 = [1, 1, 1, 1]^T$, and its initial state estimate $\hat{X}_{0|0} = [0.2019, 0.0018, 0.7446, 0.8739]^T$ is generated by a random 4×1 vector with X_0 mean, and the corresponding error covariance matrix is $P_{0|0} = 1 \times I_4$.

Three kinds of strategies for sensor coordination are conducted for target tracking: 1) the proposed sensor coordination strategy combining CTSS, MMCR, and SMIA; 2) Compared strategy 1: random sensor selection with SMIA motion strategy; and 3) Compared strategy 2: static sensor selection, which assumed that sensors cannot move and that the optimal combination of task sensors is selected by comparing all the possible combinations. The tracking trajectories are illustrated in Fig. 5. The red lines are the actual trajectory of the target, and the blue lines are the estimated trajectories by the preceding three different sensor coordination strategies. It can be seen that the proposed strategy owns the best tracking performance.

Figs. 6 and 7 compare the position errors of the three strategies. Fig. 6 shows the position deviations in a single run, and Fig. 7 shows the root-mean-square errors (RMSEs) of 200 Monte Carlo simulations. Obviously, the position estimate error of the proposed coordination strategy is the smallest among the three strategies. The reason for the advantage of Compared strategy 2 over Compared strategy 1 is that random task sensor selection cannot guarantee the optimal sensor combination, which results that the optimal movement of task sensors does not make a better tracking performance than the optimal selection of static sensors.

To validate the efficiency of CTSS and MMCR, the number of sensors and combinations at each time step is compared in a single run before and after the corresponding algorithms.

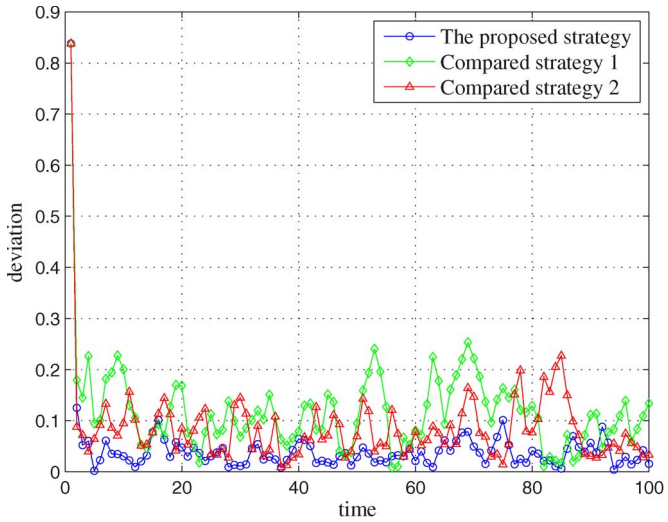

Fig. 6. Position deviation of three different strategies in a single run.

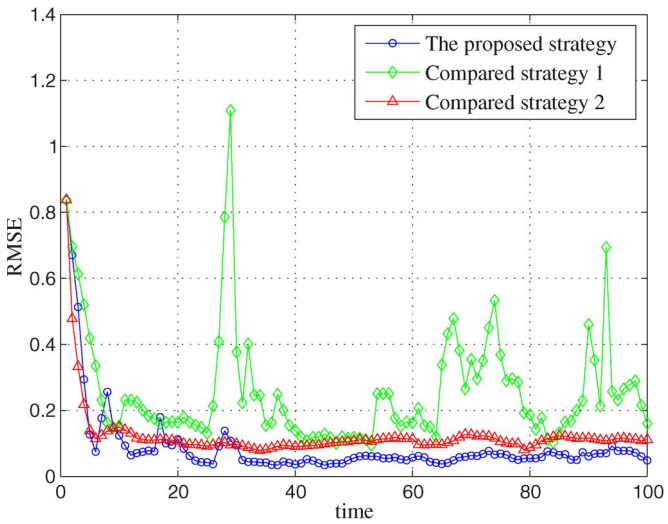

Fig. 7. RMSEs of three different strategies in 200 runs.

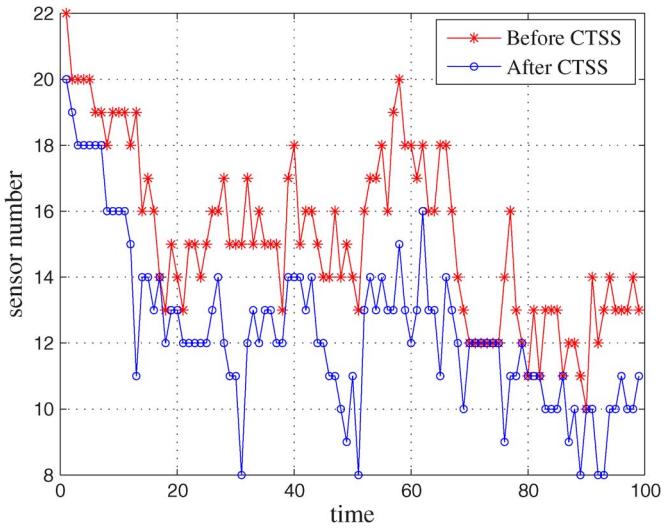

Fig. 8. Comparison between the number of sensors before and after CTSS.

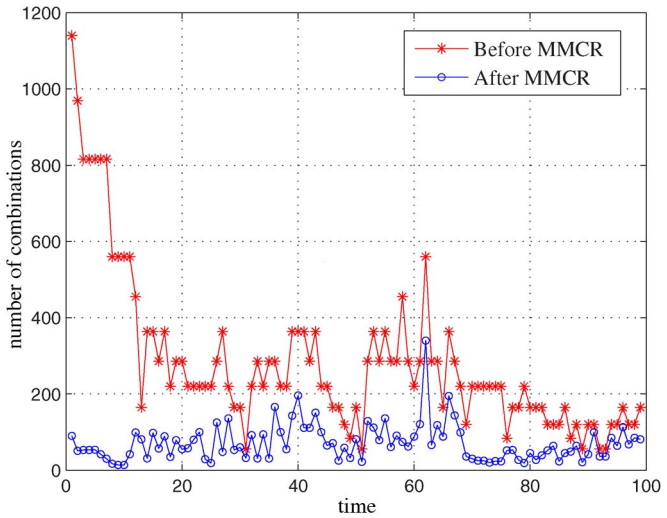

Fig. 9. Comparison between the number of combinations before and after MMCR.

From Fig. 8, it can be seen that by CTSS, the number of candidate task sensors is reduced, and the percentage of average reduction is 18.03%. One sensor reduction can bring a big reduction on sensor combinations. Fig. 9 compares the number of combinations. By MMCR, the number of combinations is largely reduced, and the percentage of average reduction is 67.42%, which simplifies the process of sensor selection to a great extent.

VIII. Conclusion and Discussion

In this paper, a coordination strategy, including sensor selection and motion, has been proposed for a range-only tracking system with mobile sensors randomly scattered. According to the properties of the tacking accuracy metric, which is derived based on the measurement model with both AMN, the search space of each sensor is reduced from a round to a curve. Then, considering the movable region of each sensor, an algorithm is designed to select the candidate task sensors at each time step, following upon an algorithm for the reduction on the number of sensor combinations. They both simplify the process of sensor selection in a great deal. An iterative algorithm is adopted to move sensors for the improvement of tracking accuracy. Simulation results illustrate the efficiency of our proposed strategy.

Our proposed coordination strategy can be extended to other cases. For the case of bearing-only sensors with AN, the FIM-based metric is also a function of sensor–target distance and angles, and a shorter distance leads to a better tracking performance, which is in the same mathematical form of the range-only sensors we considered. Therefore, our proposed coordination strategy can be easily extended to the case of bearing-only sensors. In addition, multiple target tracking is an interesting extension of our work, which will involve much more complicated problems, including data association, task assignment, and balance on sensor motion.

References

[1] X. Wang, M. Fu, and H. Zhang, "Target tracking in wireless sensor networks based on the combination of KF and MLE using distance measurements," *IEEE Trans. Mobile Comput.*, vol. 11, no. 4, pp. 567–576, Apr. 2012.

[2] S. Martínez and F. Bullo, "Optimal sensor placement and motion coordination for target tracking," *Automatica*, vol. 42, no. 4, pp. 661–668, Apr. 2006.
[3] F. Zhao, J. Shin, and J. Reich, "Information-driven dynamic sensor collaboration for tracking applications," *IEEE Signal Process. Mag.*, vol. 19, no. 2, pp. 61–72, Mar. 2002.
[4] Y. Bar-Shalom, X. Li, and T. Kirubarajan, *Estimation With Applications to Tracking and Navigation: Theory Algorithms and Software*. Hoboken, NJ, USA: Wiley, 2001.
[5] H. Wang, K. Yao, and D. Estrin, "Information-theoretic approaches for sensor selection and placement in sensor networks for target localization and tracking," *J. Commun. Netw.*, vol. 7, no. 4, pp. 438–449, Dec. 2005.
[6] X. Cao, J. Chen, Y. Xiao, and Y. Sun, "Building environment control with wireless sensor and actuator networks: Centralized vs. distributed," *IEEE Trans. Ind. Electron.*, vol. 57, no. 11, pp. 3596–3605, Nov. 2010.
[7] P. Cheng, J. Chen, F. Zhang, Y. Sun, and X. Shen, "A distributed TDMA scheduling algorithm for target tracking in ultrasonic sensor networks," *IEEE Trans. Ind. Electron.*, vol. 60, no. 9, pp. 3836–3845, Sep. 2013.
[8] R. C. Luo and T. M. Chen, "Autonomous mobile target tracking system based on grey-fuzzy control algorithm," *IEEE Trans. Ind. Electron.*, vol. 47, no. 4, pp. 920–931, Aug. 2000.
[9] H. Song, V. Shin, and M. Jeon, "Mobile node localization using fusion prediction-based interacting multiple model in cricket sensor network," *IEEE Trans. Ind. Electron.*, vol. 59, no. 11, pp. 4349–4359, Nov. 2012.
[10] A. Bishop, B. Fidan, B. Anderson, K. Doançay, and P. Pathirana, "Optimality analysis of sensor–target localization geometries," *Automatica*, vol. 46, no. 3, pp. 479–492, Mar. 2010.
[11] K. Zhou and S. Roumeliotis, "Optimal motion strategies for range-only constrained multisensor target tracking," *IEEE Trans. Robot.*, vol. 24, no. 5, pp. 1168–1185, Oct. 2008.
[12] K. Zhou and S. Roumeliotis, "Multirobot active target tracking with combinations of relative observations," *IEEE Trans. Robot.*, vol. 27, no. 4, pp. 678–695, Aug. 2011.
[13] Z. Wang and D. Gu, "Cooperative target tracking control of multiple robots," *IEEE Trans. Ind. Electron.*, vol. 59, no. 8, pp. 3232–3240, Aug. 2012.
[14] L. Kaplan, "Global node selection for localization in a distributed sensor network," *IEEE Trans. Aerosp. Electron. Syst.*, vol. 42, no. 1, pp. 113–135, Jan. 2006.
[15] L. Kaplan, "Local node selection for localization in a distributed sensor network," *IEEE Trans. Aerosp. Electron. Syst.*, vol. 42, no. 1, pp. 136–146, Jan. 2006.
[16] M. Zoghi and M. Kahaei, "Adaptive sensor selection in wireless sensor networks for target tracking," *IET Signal Process.*, vol. 4, no. 5, pp. 530–536, Oct. 2010.
[17] R. Luo and O. Chen, "Mobile sensor node deployment and asynchronous power management for wireless sensor networks," *IEEE Trans. Ind. Electron.*, vol. 59, no. 5, pp. 2377–2385, May 2012.
[18] S. Kay, *Fundamentals of Statistical Signal Processing: Estimation Theory*. Upper Saddle River, NJ, USA: Prentice-Hall, 1993.
[19] Z. Yang, C. Chan, and Y. Wang, "A high-accuracy detection and estimation method of intermodulated sinusoids," *IEEE Trans. Circuits Syst. I, Reg. Papers*, vol. 58, no. 10, pp. 2477–2484, Oct. 2011.
[20] Z. Yang and C. W. Chan, "On estimation of intermodulated frequencies for sinusoidal signals with unknown fundamental frequencies," *IEEE Trans. Signal Process.*, vol. 57, no. 8, pp. 3279–3283, Aug. 2009.
[21] D. Ucinski, "Optimal sensor location for parameter estimation of distributed processes," *Int. J. Control*, vol. 73, no. 13, pp. 1235–1248, 2000.
[22] A. Emery and A. Nenarokomov, "Optimal experiment design," *Meas. Sci. Technol.*, vol. 9, no. 6, p. 864, 1999.
[23] H. Cho and S. W. Kim, "Mobile robot localization using biased chirp-spread-spectrum ranging," *IEEE Trans. Ind. Electron.*, vol. 57, no. 8, pp. 2826–2835, Aug. 2010.

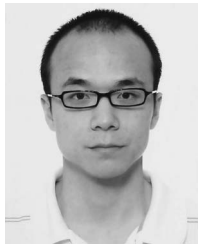

Zaiyue Yang (M'10) received the B.S. and M.S. degrees from the University of Science and Technology of China, Hefei, China, in 2001 and 2004, respectively, and the Ph.D. degree from The University of Hong Kong, Hong Kong, in 2008.

He was a Postdoctoral Fellow and a Research Associate with the Department of Applied Mathematics, The Hong Kong Polytechnic University, Kowloon, Hong Kong before joining, in 2010, Zhejiang University, Hangzhou, China, where he is currently an Associate Professor. His current research interests include smart grid, signal processing, and control theory.

Xiufang Shi received the B.Eng. degree in automation from East China University of Science and Technology, Shanghai, China, in 2011. She is currently working toward the Ph.D. degree in the Department of Control Science and Engineering, Zhejiang University, Hangzhou, China.

Her major research interests include target tracking and sensor scheduling in wireless sensor networks.

Jiming Chen (M'08–SM'11) received the B.Sc. and Ph.D. degrees in control science and engineering from Zhejiang University, Hangzhou, China, in 2000 and 2005, respectively.

He is a Full Professor with the Department of Control, Zhejiang University. His research interests are estimation and control over sensor network, sensor and actuator network, and coverage and optimization in sensor network. He has authored over 80 papers in these areas.